Indirect Determination of the ^{230}Th(n,f) and ^{231}Th(n,f) Cross Sections for Thorium-Based Nuclear Energy Systems

B.L. Goldblum,[1] S.R. Stroberg,[1] J.M. Allmond,[2] C. Angell,[1] L.A. Bernstein,[3] D.L. Bleuel,[3] J.T.Burke,[3] J. Gibelin,[4] L. Phair,[5] N.D. Scielzo,[3] E. Swanberg,[1] A. Mukherjee,[3] and E.B. Norman[1,3,5]

[1]Department of Nuclear Engineering, University of California, Berkeley, California 94720, USA
[2]Department of Physics, University of Richmond, Virginia 23173, USA
[3]Lawrence Livermore National Laboratory, Livermore, California 94551, USA & Arizona State University, Dept. of Earth & Space Exploration, Tempe, AZ, USA
[4]GANIL (DSM-CEA/IN2P3-CNRS), B. P. 55027, F-14076 Caen Cedex 5, France
[5]Nuclear Science Division, Lawrence Berkeley National Laboratory, Berkeley, California 94720, USA

(Dated: October 11, 2021)

Indirect Determination of the ^{230}Th(n,f) and ^{231}Th(n,f) Cross Sections for Thorium-Based Nuclear Energy Systems

B.L. Goldblum,[1] S.R. Stroberg,[1] J.M. Allmond,[2] C. Angell,[1] L.A. Bernstein,[3] D.L. Bleuel,[3] J.T. Burke,[3] J. Gibelin,[4] L. Phair,[5] N.D. Scielzo,[3] E. Swanberg,[1] A. Mukherjee,[3] and E.B. Norman[1, 3, 5]

[1]*Department of Nuclear Engineering, University of California, Berkeley, California 94720, USA*
[2]*Department of Physics, University of Richmond, Virginia 23173, USA*
[3]*Lawrence Livermore National Laboratory, Livermore, California 94551, USA & Arizona State University, Dept. of Earth & Space Exploration, Tempe, AZ, USA*
[4]*GANIL (DSM-CEA/IN2P3-CNRS), B. P. 55027, F-14076 Caen Cedex 5, France*
[5]*Nuclear Science Division, Lawrence Berkeley National Laboratory, Berkeley, California 94720, USA*
(Dated: October 11, 2021)

The Surrogate Ratio Method (SRM) was employed in the first experimental determination of the ^{231}Th(n,f) cross section, relative to the ^{235}U(n,f) cross section, over an equivalent neutron energy range of 360 keV to 10 MeV. The ^{230}Th(n,f) cross section was also deduced using the SRM, relative to the ^{234}U(n,f) cross section, over an equivalent neutron energy range of 220 keV to 25 MeV. The desired compound nuclei were populated using (^{3}He,^{3}He) and (^{3}He,α) reactions on targets of ^{232}Th and ^{236}U and relative fission decay probabilities were measured. The surrogate ^{230,231}Th(n,f) cross sections were compared to cross section evaluations and directly-measured experimental data, where available.

I. INTRODUCTION

The thorium-uranium fuel cycle has several advantages, with respect to nonproliferation and radioactive waste management, when compared with the conventional uranium-plutonium fuel cycle [1]. In a fast spectrum breeder reactor, neutron capture on natural thorium (^{232}Th, monoisotopic) followed by beta decay gives rise to an excess of fissile nuclear material (^{233}U). The fissile material in thorium-based fuels is thus created *in situ*, obviating the need for enrichment technology, which presents dual-use scenarios (i.e., enrichment technology can be used for the production of both reactor-grade and weapons-grade fuel). Further, in a thorium-based fuel cycle, the quantity of minor actinides in the radioactive waste stream is reduced by 2-3 orders of magnitude when compared with the uranium-plutonium fuel cycle [2].

Although the concept for a thorium-based fuel cycle is not new, much of the experimental nuclear data required for design calculations for thorium-based reactor systems are not precise or even absent. To achieve improved design calculations for thorium-based reactors, the determination or reevaluation of neutron-induced reaction cross sections on isotopes of thorium is required [3]. Little data exist on the ^{230}Th(n,f) cross section in the energy range relevant for fast reactor systems with poor agreement between the measurements. Direct measurement of the ^{231}Th(n,f) cross section is difficult given the short half-life of the target ($t_{1/2}$ = 25.52 h) [4].

To overcome the experimental limitations associated with direct neutron-induced reaction cross section measurements, several indirect methods for the determination of neutron-induced reaction cross sections have been developed and successfully benchmarked [5]. The Surrogate Method is one such technique whereby neutron-induced reaction cross sections can be extracted on both stable and radioactive nuclei [6]. This is accomplished by measuring the relevant decay probability for the same compound nucleus formed in the neutron-induced reaction, but produced using a light-ion-induced direct reaction using a stable target and beam.

There are two means of application of the Surrogate Method, the absolute probability approach, or absolute surrogate technique, and the relative probability approach, or surrogate ratio method (SRM). Using the external SRM, the same surrogate direct reaction is performed on two similar targets (e.g., in mass, deformation, etc.) and a ratio of the experimentally determined surrogate-fission probabilities for two different compound nuclei is determined [7–10]. This ratio, a stand-in for the ratio of neutron-induced fission probabilities, is then multiplied by a fiducial neutron-induced reaction cross section to obtain the neutron-induced reaction cross section of interest. By tailoring the experiment such that the total number of direct reaction events on the two target nuclei are equal within an excitation-energy-independent factor, the SRM removes the need to measure these quantities, thus eliminating what is often the largest source of systematic uncertainty in surrogate measurements.

The ^{230}Th(n,f) and ^{231}Th(n,f) cross sections were determined using the SRM relative to the well-measured ^{234}U(n,f) and ^{235}U(n,f) cross sections, respectively. In Table I, the surrogate reactions (Column 1) used to produce the compound nuclei of interest (Column 2) are listed. The current experimental uncertainty for the corresponding neutron-induced fission cross sections (Column 3) in the energy range relevant for fast reactor systems is given in Column 4 of Table I. The uncertainty in the ^{235}U(n,f) cross section was obtained by averaging the uncertainty given in the Evaluated Nuclear Data File (ENDF/B-VII.0) covariance matrix over the neutron energy range of 1 MeV to 20 MeV [11]. Uncer-

TABLE I: Summary of Reactions and Pertinent Information for the ^{230,231}Th(n,f) Surrogate Cross Section Measurements

Surrogate Reaction	Compound Nucleus	Neutron-Induced Reaction	Initial uncertainty in $\sigma_{(n,f)}$ (%)
$^{232}_{90}$Th($^3_3$He,α) ,	$^{231}_{90}$Th	$^{230}_{91}$Th(n,f)	15
Th(He, He)	Th	Th(n,f)	Insufficient Data
^{236}U(^{3}He,α)	^{235}U	^{234}U(n,f)	3
^{236}U(^{3}He,^{3}He′)	^{236}U	^{235}U(n,f)	1

tainties in the ^{235}U(n,f) and ^{230}Th(n,f) cross section data were estimated by evaluating the spread between the ENDF/B-VII.0 and Japan Evaluated Nuclear Data Library (JENDL-3.3) evaluations in the energy range of 1 MeV to 20 MeV. It is important to note, however, that deviations in the experimental ^{230}Th(n,f) cross section data of up to 200% were present when compared to the ENDF/B-VII.0 and JENDL-3.3 evaluations in this energy range. For the ^{231}Th (n,f) cross section, no experimental data is available and the single evaluation from the Russian file of evaluated neutron data (ROSFOND) prevents an estimation of the initial uncertainty in the evaluation. To the benefit of future nuclear energy systems, we present here a measurement of the ^{230}Th(n,f) and ^{231}Th(n,f) cross sections, formerly a major source of uncertainty in thorium-based reactor design calculations, to within an average total estimated uncertainty of approximately 10% in the neutron energy range relevant for fast reactor systems.

In Sec. II, an outline of the experimental procedure is given. The surrogate ^{230}Th and ^{231}Th neutron-induced fission cross sections are discussed in Secs. III A and III B, respectively. A detailed analysis of the uncertainty associated with the measurement is given in Sec. III C. Finally, concluding remarks are given in Sec. IV.

II. EXPERIMENTAL METHOD

A 42-MeV ^{3}He^{2+} beam from the 88–Inch Cyclotron at Lawrence Berkeley National Laboratory was employed in the experiment. Data were taken over a period of 3 days with a beam intensity of approximately 1 enA. The ^{232}Th target, of isotopic purity $\approx$ 99.99%, was a self-supporting metallic foil with a thickness of 889 $\pm$ 45 μg/cm^2, as determined using α particle energy loss measurements. The ^{236}U target of 184 $\pm$ 5 μg/cm^2 thickness, as measured by α particle counting, was prepared by electroplating uranium onto a 2.29 mg/cm^2 Ta foil. The isotopic composition of the ^{236}U target was 99.7% ^{236}U and 0.3% ^{234}U.

The reaction products were detected using the Silicon Telescope Array for Reaction Studies (STARS) and associated electronics, as described Ref. [9]. STARS was comprised of a particle telescope consisting of two double-sided Micron Semiconductor S2 type silicon detectors (22 mm active inner diameter and 70 mm active outer diameter), a 150 μm ΔE detector and a 994 μm E detector, covering a forward angle range of 36° to 67° relative

to the beam axis. The ΔE and E detectors were spaced approximately 3 mm apart. The targets were located approximately 15 mm upstream from the front face of the ΔE detector. A 4.44 mg/cm^2 aluminum foil, biased to 300 V to mitigate the effect of δ electrons, was placed between the target and STARS to prevent damage to the detector caused by forward flying fission fragments. Fission fragments were detected in a 140 μm Micron S2 detector located approximately 13 mm upstream from the target. The fission detector covered an angle range of 110° to 139° relative to the beam axis. Each silicon detector had a 1000 angstrom aluminum front and a 3000 angstrom gold backing for electrode contact, and was segmented into the electrical equivalent of 24 rings on one side and 8 sectors on the other side. The ΔE, E and fission detectors were biased with 22 V, 150 V and 40 V, respectively, and the master-trigger rate ranged between 6 and 10 kHz during the experiment. The particle-fission timing was obtained using a time-to-amplitude converter (TAC) module digitized by an Ortec AD413 peak-sensing analog-to-digital converter.

As previously described [10], the unknown cross section, $\sigma^{(1)}_{n,f}$ is determined using the SRM relative to some well-measured cross section, $\sigma^{(2)}_{n,f}$, as a function of excitation energy, E, via the following expression:

$$\sigma^{(1)}_{n,f}(E) = \kappa \frac{\varrho^{(2)}_f(E) N^{(1)}_{\delta f}(E)}{\varrho^{(1)}_f(E) N^{(2)}_{\delta f}(E)} \sigma^{(2)}_{n,f}(E). \qquad (1)$$

Here, the superscripts (1) and (2) denote the two compound nuclei employed in the ratio. The surrogate reaction is denoted by δ and $N_{\delta f}$ is the number of direct reaction ejectiles in coincidence with fission. The efficiency for detecting the fission exit channel is ϱ_f and the excitation-energy-independent parameter κ is given by

$$\kappa = \frac{\rho^{(2)} \int_0^{\Delta t^{(2)}} I^{(2)}\ell^{(2)}dt}{\rho^{(1)} \int_0^{\Delta t^{(1)}} I^{(1)}\ell^{(1)}dt}, \qquad (2)$$

where ρ represents the areal target density, I is the beam intensity delivered to the target in particles per unit time, ℓ is the live time fraction of the data acquisition system and Δt is the elapsed time for data collection.

The areal density of the ^{232}Th and ^{236}U targets was determined, as described above. The beam intensity was obtained by continuously measuring the current delivered to a Faraday cup. The live time fraction of the data acquisition system was determined from the ratio
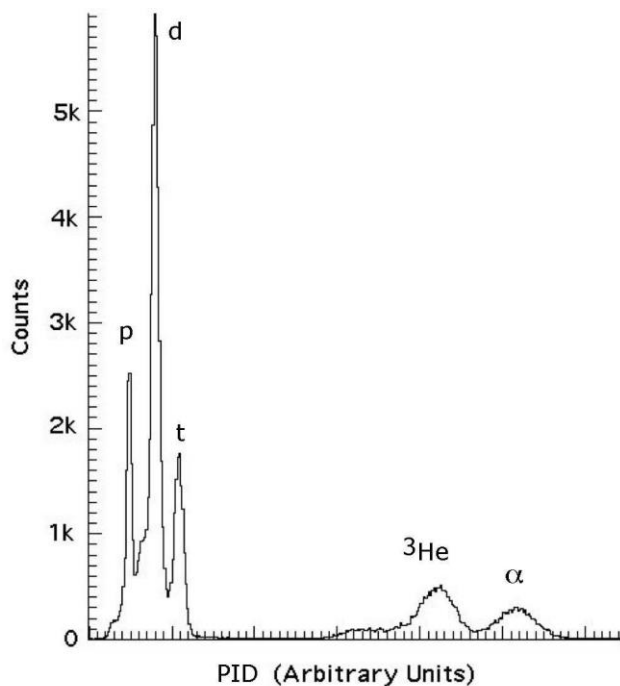
FIG. 1: Representative particle identification spectrum for direct reaction ejectiles in coincidence with fission, with prompt timing identified by a peak in the TAC spectrum, obtained from 42 MeV ^{3}He particles incident on the ^{232}Th target. From left to right, the peaks correspond to protons, deuterons, tritons, ^{3}He particles and α particles. The low energy shoulder on the ^{3}He-particle peak is attributed to incomplete charge collection in the particle telescope.

of the number of master trigger events to the number of digitized events and was typically between 60 and 75%. Given the tantalum target backing, the time elapsed for data collection on the ^{236}U target was approximately twice as long as that for the ^{232}Th target. The κ parameter is the same for the two surrogate cross section measurements described herein and was determined to be 0.32 ± 0.02.

III. DATA ANALYSIS AND RESULTS

A single signal in one ring and one sector of both silicon detectors was required for a valid event. However, event reconstruction was accomplished in the cases in which a particle traversed two rings when passing through a detector, leaving a fraction of its energy in each, or in the case of induced charge on adjacent electrodes. Particle identification was performed by linearizing the energy deposited in the particle telescope [12], as illustrated in Fig. 1. The particle identification (PID) is then given by

$$PID = [(\Delta E + E)^{1.7} - E^{1.7}] \cos \vartheta, \quad (3)$$

where ΔE is the energy deposited in the ΔE detector, E is the energy deposited in the E detector and ϑ is the

polar angle of detection of the ejectile with respect to the beam axis, as determined by the ring identification number in the ΔE detector. Using linearized ^{3}He and alpha particle identification, the total energy of the ejectile was reconstructed from the sum of the ΔE and E detector energies as well as calculations of energy losses from target recoil and in the aluminum shield and aluminum and gold layers of the silicon detectors. From the known reaction kinematics, the excitation energy of the compound nuclei are calculated from the reconstructed surrogate reaction ejectile energy. Incomplete charge collection in the particle telescope resulted in a clearly discernible low-energy tail on the ^{3}He-particle peak (See Fig. 1.). It is assumed that any potential contribution from incomplete charge collection on the α particle peak that enters into the ^{3}He-particle gate is the same for the two target nuclei employed in the measurement and thus cancels in the ratio analysis. Using the detector at back angles relative to the beam axis as a tag for the fission exit channel, the number of particle-fission coincident events as a function of excitation energy was obtained for each compound nucleus relevant for the surrogate ratio measurements.

An enhancement in the efficiency for detecting fission could arise from a forward-peaked fission fragment angular distribution [13]. To determine if anisotropies existed in the fission fragment angular distributions that affect the excitation-energy-dependent fission detection efficiency, $\varrho_f(E)$, for each compound nucleus employed in the ratio, the sector segmentation of the ΔE and fission detectors was utilized to explore the angular correlation of the fission events with respect to the plane defined by the beam and the detected direct reaction ejectile. A fission fragment enhancement factor (EF) was extracted from the data, defined as the number of in-plane fission events relative to the number of out-of-plane events, corrected for geometric factors arising from detector segmentation. If anisotropy exists in the fission fragment angular distribution, the enhancement factor is expected to deviate from unity. However, if the deviation from isotropy is similar for the two compound nuclei employed in the ratio measurement, no correction to the fission detection efficiency is necessary. The enhancement factors for detecting fission of the two compound nuclei were equal within experimental uncertainty over the entire excitation energy range probed, and thus no correction for fission fragment anisotropy was applied in the ratio analysis.

A. ^{230}Th(n,f) Cross Section

To obtain the ^{230}Th(n,f) cross section shown in Fig. 2, the normalized ratio of the number of particle-fission coincident events for the ^{231}Th and ^{235}U compound nuclei accessed via the (^{3}He,α) pickup reaction was multiplied by the ENDF/B-VII.0 ^{234}U(n,f) cross section matched at excitation energy and the result was shifted into equivalent neutron energy by subtracting the neu-
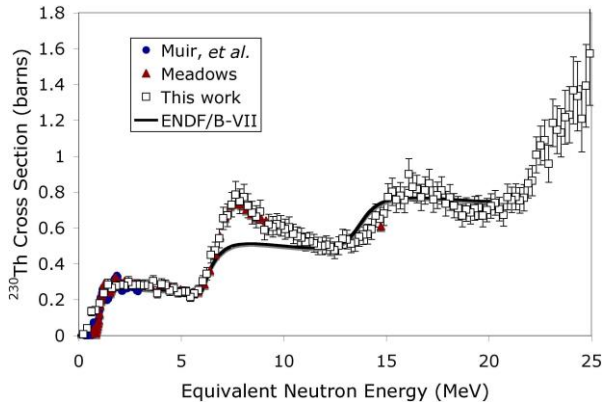
FIG. 2: (Color online) The ^{230}Th(n,f) cross section in the equivalent neutron energy range of 0 to 25 MeV. The error bars on the surrogate data represent both the statistical and non-statistical uncertainty. For comparison, evaluated and directly-measured ^{230}Th(n,f) cross section data are shown.

FIG. 3: (Color online) The ^{230}Th(n,f) cross section in the equivalent neutron energy range of 0 to 5 MeV. The error bars on the surrogate data represent both the statistical and non-statistical uncertainty. For comparison, evaluated and directly-measured ^{230}Th(n,f) cross section data are shown.

tron separation energy of the ^{231}Th compound nucleus (S_n = 5.118 MeV) from the excitation energy. The shape of the surrogate ^{230}Th(n,f) cross section trends well with the evaluated ^{230}Th(n,f) cross section from ENDF/B-VII.0 and with directly-measured data from Meadows [14] and Muir, *et al.* [15] from 1 MeV to approximately 6 MeV equivalent neutron energy. The low energy region is discussed in more detail below. Near the onset of second chance fission (i.e., (*n, nf*)), the surrogate cross section substantially deviates from the evaluation, but is in good agreement with the experimental data from Meadows. The surrogate data converge with the evaluated result at 11 MeV equivalent neutron energy, but then exhibit a slight discrepancy beyond the third chance fission threshold. From 15 MeV to 20 MeV equivalent neutron energy, the surrogate cross section agrees with the evaluated result within the total estimated uncertainty. The surrogate result extends to the onset of fourth chance fission at approximately 25 MeV equivalent neutron energy.

An expansion of the ^{230}Th(n,f) cross section data in the low equivalent neutron energy range is given in Fig. 3. Data for excitation energies at or below 5320 keV were not plotted because the 200-keV energy bin overlaps with negative equivalent neutron energy for *n*+^{230}Th. A significant deviation between the surrogate cross section and the evaluated and experimental data is observed below 1 MeV equivalent neutron energy. In the Weisskopf-Ewing limit [16], a fundamental assumption of the SRM, the decay probabilities are independent of the total angular momentum and parity of the populated states. The discrepancy at low energy may suggest a breakdown of the Weisskopf-Ewing approximation in this energy range. Low energy resonances near 700 keV, 1.2 MeV and 1.8 MeV observed in the Meadows and Muir, *et al.*, directly-measured data are not resolved in this work.
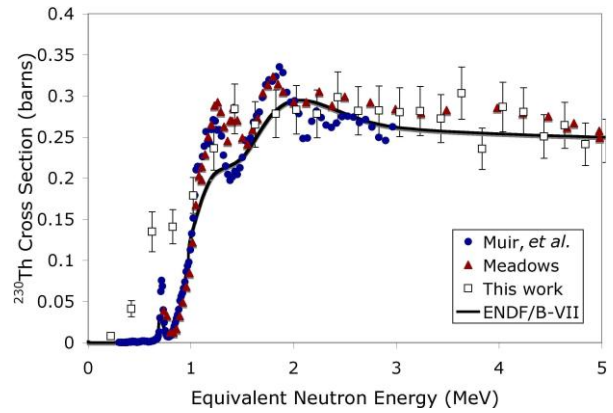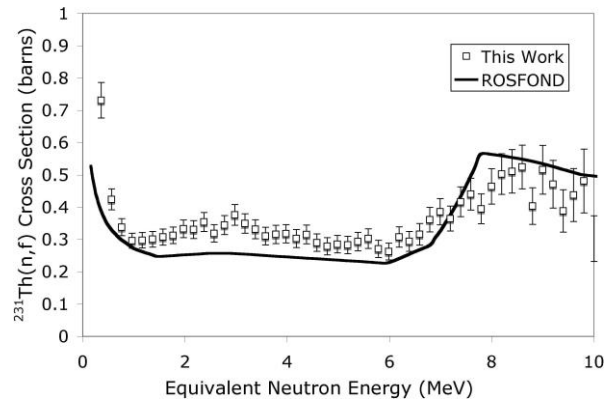

FIG. 4: The ^{231}Th(n,f) cross section extracted using the SRM, relative to the evaluated ^{235}U(n,f) cross section obtained from ENDF/B-VII.0, as a function of equivalent neutron energy is given by the open squares. The error bars represent both the statistical and non-statistical uncertainty. For comparison, the evaluated ^{231}Th(n,f) cross section from ROSFOND is denoted by the solid line.

B. ^{231}Th(n,f) Cross Section

The first experimental determination of the ^{231}Th(n,f) cross section is shown in Fig. 4. This result was obtained by multiplying the normalized ratio of the number of particle-fission coincident events for the ^{232}Th and ^{236}U compound nuclei accessed via the (^{3}He,^{3}He′) inelastic scattering reaction by the evaluated ^{235}U(n,f) cross section obtained from ENDF/B-VII.0 matched at excitation energy. The result was shifted into equivalent neutron energy by subtracting the neutron separation energy of the ^{232}Th compound nucleus (S_n = 6.438 MeV) from the excitation energy. The surrogate data is compared with the

evaluated ^{231}Th(n,*f*) cross section obtained from ROS-FOND.

Data for excitation energies at or below 6640 keV were not plotted because the 200-keV energy bin overlaps with negative equivalent neutron energy for *n*+^{231}Th. The shape of the ^{231}Th(n,*f*) cross section at low energy suggests that the fission barrier, B_f , of ^{231}Th is lower than the neutron separation energy in the ^{232}Th compound nucleus, consistent with the prediction of Vandenbosch and Huizenga of B_f = 6.2 $\pm$ 0.2 [17]. In the equivalent neutron energy range of approximately 1 MeV to 7 MeV, the surrogate ^{231}Th(n,*f*) cross section data are systematically higher than the ROSFOND evaluation. Near the onset of second chance fission, the surrogate cross section data and the evaluation agree, however, the ^{231}Th(n,*f*) surrogate cross section data exhibit a more gradual rise than is indicated in the evaluation. Above 10 MeV equivalent neutron energy, the surrogate ^{231}Th(n,*f*) cross section result is plagued by poor statistics, with statistical uncertainties much greater than 30%.

C. Uncertainty Analysis

A detailed uncertainty analysis was performed for the energy and cross section data. The surrogate ejectile energy data were grouped into energy bins in 200 keV increments from zero to the maximum energy of the ejectile. To determine the energy centroid of the 200 keV bin, energy data were further subdivided into 40 keV bins and a weighted mean of the energy was extracted. The standard deviation of the mean was negligible for all energy bins and thus smaller than the size of the data points for all figures in this text.

For the energy data (*x*-axis), sources of non-statistical uncertainty and their associated error are listed in Table II. The energy straggle arose from statistical fluctuations of the specific energy loss of the direct reaction ejectile as it traversed the aluminum and gold layers on the silicon detectors, and the aluminum shield. Energy loss in the target, aluminum shield and aluminum and gold electrode layers were calculated using the Energy Loss and Straggling Tool (ELAST) [18]. The energy loss calculations were performed as a function of the angle at which the particle traversed the material, as determined by the ring identification number in the ΔE detector. Uncertainty in the target-detector spacing of ±0.5 mm and an angular resolution between 0.8° and 2.4° resulted in an uncertainty in the angle of detection of the ejectile and thus an uncertainty in the energy loss calculations. The intrinsic detector resolution was measured using a ^{226}Ra alpha source. The 60 keV cyclotron beam energy resolution was measured in a previous experiment [8]. The total uncertainty from Table II compares well with the observed 204 keV 1σ standard deviation of the 42 MeV ^{3}He elastic peak from this experiment. Based on this and the values listed in Table II, an appropriate value for the energy uncertainty in the final extracted cross sections

TABLE II: The 1σ uncertainty in the energy data. The range given for some values is a result of angular resolution of the segmented rings in the particle telescope.

Source	ΔE (keV)
Energy Straggle	36 - 59
Energy Loss Calculations	18 - 40
Intrinsic Detector Resolution	190
Cyclotron Beam	60
Total Uncertainty	203 - 212

TABLE III: Uncertainty in the surrogate cross section data.

Source	Uncertainty (%)
^{232}Th Target Thickness	5
^{236}U Target Thickness	3
Average Beam Intensity	< 1
Average Live Time Fraction	< 1
Elapsed Time for Data Collection	< 1
Fission Tagging Efficiency	3
^{235}U(n,*f*) Cross Section	1
^{234}U(n,*f*) Cross Section	3

was taken to be 212 keV for all bins.

The sources of non-statistical uncertainty in the cross section data (*y*-axis) for the surrogate ratio measurement are summarized in Table III. The systematic uncertainty is dominated by the uncertainty in the κ parameter (See Eq. 2.). For the surrogate ^{230}Th(n,*f*) cross section, the statistical uncertainty ranges from 6% to 28% over the equivalent neutron energy range of 220 keV to 25 MeV. For the surrogate ^{231}Th(n,*f*) cross section, the statistical uncertainty ranges from 4% to 22% over the equivalent neutron energy range of 360 keV to 10 MeV. This results in a total average uncertainty for both the ^{230}Th(n,*f*) and ^{231}Th(n,*f*) cross sections obtained using the SRM over the entire equivalent neutron energy range of approximately 10.5%.

IV. CONCLUSION

The first experimental determination of the ^{231}Th(n,*f*) cross section was performed using the SRM. General agreement of the surrogate ^{230}Th(n,*f*) cross section with directly-measured and evaluated data suggest that the underlying assumptions of the surrogate ratio methodology are borne out in the analysis. The data extracted from the experiments outlined here will improve the accuracy of thorium-based reactor design calculations that require neutron-induced fission cross section input data. This work suggests that the SRM can be successfully applied in the future to extract (n,*f*) cross section data on radioactive nuclei - essential for the adequate benchmarking of advanced thorium-based nuclear reactor systems.

[1] D.N. Suglobov, R.M. Yakovlev and B.F. Myasoedov, Radiochemistry, 49, 441 (2007).

[2] B. Haas, Brazilian J Phys, 34, 814 (2004).

[3] A. Kumar, U. Kannan, R. Srivenkatesan, Ann. Nucl. Energy 29, 1967 (2002).

[4] *Table of Isotopes*, 8th ed., edited by R.B. Firestone and [5] S. Shirley (Wiley, New York, 1996), Vol. II.

[6] J. Escher and F.S. Dietrich, in *Reaction Mechanisms for Rare Isotope Beams: Second Argonne/MSU/JINA/INT RIA Workshop, Michigan State University, East Lansing, 2005*, edited by B.A. Brown (American Institute of Physics, 2005), p. 93.

[7] J.D. Cramer and H.C. Britt, Nucl. Sci. Eng. 41, 177 (1970).

[8] C. Plettner, H. Ai, C.W. Beausang, L.A. Bernstein, L. Ahle, H. Amro, M. Babilon, J.T. Burke, J.A. Caggiano, R.F. Casten, *et al.*, Phys. Rev. C 71, 051602(R) (2005).

[9] J.T. Burke, L.A. Bernstein, J. Escher, L. Ahle, J.A. Church, F.S. Dietrich, K.J. Moody, E.B. Norman, L. Phair, P. Fallon, *et al.*, Phys. Rev. C 73, 054604 (2006).

[10] B.F. Lyles, L.A. Bernstein, J.T. Burke, F.S. Dietrich, J. Escher, I. Thompson, D.L. Bleuel, R.M. Clark, P. Fallon, J. Gibelin, *et al.*, Phys. Rev. C 76, 014606 (2007).

[11] S.R. Lesher, J.T. Burker, L.A. Bernstein, H. Ai, C.W. Beausang, D.L. Bleuel, R.M. Clark, F.S. Dietrich, J.E. Escher, P. Fallon, *et al.*, Phys. Rev. C 79, 044609 (2009).

[12] M.B. Chadwick, P. Oblozinsky, M. Herman, N.M. Greene, R.D. McKnight, D.L. Smith, P.G. Young, R.E. MacFarlane, G.M. Hale, S.C. Frankle, *et al.*, "ENDF/B-VII.0: Next Generation Evaluated Nuclear Data Library for Nuclear Science and Technology," *Nuclear Data Sheets*, 107, pp. 2931-3060, 2006.

[13] F.S. Goulding and D.A. Landis, "Recent Advances in Particle Identifiers at Berkeley," in *Semiconductor Nuclear-Particle Detectors and Circuits*, Publication 1593, National Academy of Sciences, Washington, DC, 1969, p. 757.

[14] R. Vandenbosch and J.R. Huizenga. *Nuclear Fission.* (Academic Press, New York, 1973), Ch. XIV.

[15] J.W. Meadows, Argonne National Laboratory Report No. 83, 1979; J.W. Meadows, Ann. Nucl. Energy 15, 421 (1988).

[16] D.W. Muir and L.R. Veeser, in Proceedings of the Third International Conference on Neutron Cross Sections and Technology, Knoxville, 1971, Report CONF-710301, Vol. 1, p. 292; D.W. Muir and L.R. Veeser, Los Alamos Scientific Laboratory Report No. LA-4648-MS.

[17] V.F. Weisskopf and D.H. Ewing, Phys. Rev. 57, 472 (1940).

[18] R. Vandenbosch and J.R. Huizenga, *Nuclear Fission* (Academic Press, New York, 1973), p. 255.

[19] Energy loss and Straggling Tool, [Adapted from the computer program ENELOSS, written by H. Ernst (1981) with stopping power routines by K. Lesko (1984).]

DISCLAIMER

This document was prepared as an account of work sponsored by the United States Government. While this document is believed to contain correct information, neither the United States Government nor any agency thereof, nor The Regents of the University of California, nor any of their employees, makes any warranty, express or implied, or assumes any legal responsibility for the accuracy, completeness, or usefulness of any information, apparatus, product, or process disclosed, or represents that its use would not infringe privately owned rights. Reference herein to any specific commercial product, process, or service by its trade name, trademark, manufacturer, or otherwise, does not necessarily constitute or imply its endorsement, recommendation, or favoring by the United States Government or any agency thereof, or The Regents of the University of California. The views and opinions of authors expressed herein do not necessarily state or reflect those of the United States Government or any agency thereof or The Regents of the University of California.